Energies **2015**, *8*, 4118-4137; doi:10.3390/en8054118

OPEN ACCESS

energies

ISSN 1996-1073

www.mdpi.com/journal/energies

Article

A Numerical Study on Combustion and Emission Characteristics of a Medium-Speed Diesel Engine Using In-Cylinder Cleaning Technologies

Shuang He, Bao-Guo Du, Li-Yan Feng, Yao Fu, Jing-Chen Cui and Wu-Qiang Long *

Institute of Internal Combustion Engine, Dalian University of Technology, Dalian 116024, China; E-Mails: sshe_dut@163.com (S.H.); dubg@dlut.edu.cn (B.-G.D.); fengli@dlut.edu.cn (L.-Y.F.); fuyao0728@sina.com (Y.F.); cuijingchen@163.com (J.-C.C.)

* Author to whom correspondence should be addressed; E-Mail: longwq@dlut.edu.cn; Tel./Fax: +86-411-8470-8246 (ext. 207).

Academic Editor: Chang Sik Lee

Received: 26 January 2015 / Accepted: 30 April 2015 / Published: 8 May 2015

Abstract: In order to clarify the potential of internal purification methods on medium speed diesel engines to meet the IMO Tier III nitrogen oxide (NO_x) emission regulations, combined 1-D engine working cycle simulation and 3-D CFD simulation were conducted to predict the performance and emissions of the engine under different valve close timings, geometric compression ratios, injection timings, and Exhaust Gas Recirculation (EGR) rates. The numerical results show that, as the inlet valve close timing is advanced, NO_x is reduced by as much as 27%, but the peak of premixed combustion heat release rate is increased; this can weaken the ability to reduce NO_x with the Miller cycle. Moreover, the peak of premixed combustion heat release rate is reduced when the geometric compression ratio is increased to 15.4, and linking with injection timing by delaying 6°CA can further reduce NO_x by 55.3% from the baseline. Finally, over 80% NO_x reduction can be achieved when the above schemes are combined with over 15% EGR. The NO_x and soot can be reduced simultaneously by using moderate Miller cycle combination with moderate EGR, and the results show a large reduction of NO_x and moderate reduction of soot. This can be a feasible technical solution to meet Tier III regulations.

Keywords: medium-speed diesel engine; Miller cycle; EGR; NO_x emissions; numerical simulation

---

1. Introduction

Due to the increase in traffic volume, host tonnage and the quantity of marine diesel engine growing year by year, their emissions cause serious harm to the ecological environment. This issue has been of high concern for the international maritime organization (IMO), the international maritime environmental protection committee, the world health organization, and other agencies and governments. On October 10, 2008, the Maritime Environment Protection Committee (MEPC) defined three levels of IMO Marine diesel engine emission regulation systems. The Tier II emission regulation has already been implemented since 2011, and the Tier III emission regulation will apply to the emission control areas from January 1, 2016. The Tier III emission regulation requires 80% of nitrogen oxide (NO_x) reduction compared to Tier I emission regulations, which is clearly a huge change for the development of marine engines. Furthermore, the future coexistence of IMO Tier II and IMO Tier III emission areas will enhance the requirements for the flexibility of engine operation.

The major marine diesel engine manufacturers have been carrying out researches on emissions reduction, aimed at seeking the most effective and feasible technical route for the Tier III emission regulation. Various techniques, such as selective catalytic reduction (SCR), exhaust gas recirculation (EGR), humidification, and natural gas engines, have been thoroughly researched [1–4]. SCR and gas engine are the only feasible technical solutions at present. The life cycle cost of the aforementioned technologies was evaluated by Christer Wik [5], and the results show that two-stage turbocharging, dual fuel and SCR technology have more potential. However, by reason of the uncertainty of the market price of fuel and urea (the raw material of SCR system) in the future, it is difficult to make a final choice at the present stage, and there are still problems with the layout of SCR devices. In addition, other combination of the potential technical routes are proposed: Wetpac (intake humidifying/emulsified oil/water in-cylinder) + EGR + 2 TC (two-stage turbocharging), is worth further evaluation.

In view of diesel engine combustion, how to reduce NO_x and PM (particulate matter) simultaneously is a highly complicated problem. These two kinds of pollutants are formed simultaneously in traditional diesel engines which are operated with a heterogeneous mixture under conditions of high temperature burning. Shown in Figure 1, soot, the major composition of PM, is produced in the 1800–2500 K region with rich fuel conditions; NO_x emissions are produced in rich O_2 conditions with temperature higher than 2300 K. A number of researches have demonstrated that NO_x and soot emissions can be suppressed at the same time by controlling combustion temperature and the equivalent ratio φ by the new combustion concept, such as LTC (low temperature combustion) [6–8], HCCI (homogeneous charge compression ignition) [9,10] and so on. There is also a desirable path [11] in the φ-T map in which NO_x and soot can both be reduced, which is a long and narrow channel with high temperature and a rich mixture.

The Miller cycle is a low cost and effective method to reduce NO_x emissions. By advancing or delaying intake valve closing time, the effective compression ratio is decreased, and accordingly the in-cylinder compression terminal temperature and maximum combustion temperature are reduced. However, as the result of a shorter inlet valve open period, a turbocharger with higher pressure ratio (>9) is needed to compensate for the loss of intake air. Thus the air-fuel ratio is maintained so that it is consistent with the baseline engine. At the same time, the Miller cycle can improve the engine efficiency by 4%–8%. Further, in part load condition, the Miller cycle will be restricted by the thermal load, thus impairing

the ability to reduce NO_x emissions. Compared with traditional single-stage turbocharging diesel engines, extreme Miller timing technology, which advances the intake valve closing timing by 100°CA, combined with two-stage turbocharging can reduce NO_x emissions by 40%–50%.

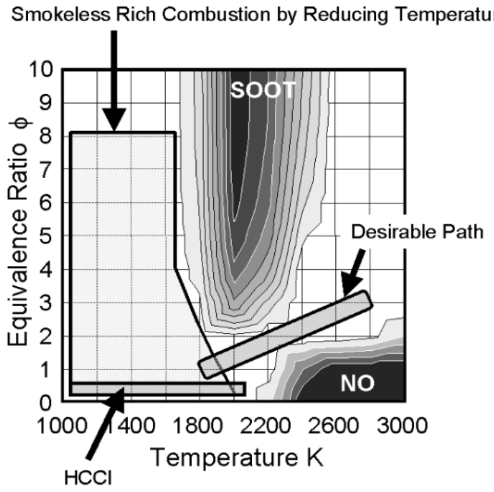

Figure 1. Comparison between new combustion concepts on a Φ-T map [7].

EGR technology [6,12–15], is namely, recirculating the cooled exhaust gas back into the combustion chamber. On the one hand, the heat capacity of the in-cylinder charge is improved, so the flame temperature can be reduced at the inlet CO_2 and water vapor; on the other hand, NO_x formation is effectively restrained by reducing the inlet concentration of O_2, slowing down the mixing speed of air and fuel, and obtaining a lower flame temperature. EGR technology demonstrates the potential of reducing NO_x emissions by 60% on the basic of the IMO Tier I emission level.

Several researches have confirmed that the combination of Miller cycle, two-stage turbocharging, and EGR technology is a feasible route to meet the IMO Tier III NO_x regulations. F. Millo *et al.* [15] established four models for EGR connection schemes on a Wärtsilä W20L6 four-stroke diesel engine by using a one dimensional CFD simulation code. EGR rate schemes of 5%–20% were simulated, and exhaust emissions and economy levels of different schemes were analyzed. The study found that, compared with single-stage turbocharging diesel engines, using 20% EGR combined with extreme Miller timing (100°CA BBDC) NO_x emissions can be reduced by 90%, while the fuel consumption rate is slightly elevated. The effects of 0%–20% EGR operation on a six-cylinder medium speed diesel engine were investigated in reference [16] by R. Verschaeren, reductions of up to 70% of NOx were attained at different loads. The greatest NOx reduction was achieved with Miller timing. It can be concluded that the EGR system is an essential part of an engine concept in order to fulfill IMO Tier III NO_x requirements, but only one Miller IVC (20°CA BBDC) was tested in his paper. In reference [17], a 1.8 l single-cylinder diesel engine was studied by Jesús Benajes by combining direct experimental data with the detailed information on the local in-cylinder conditions obtained from 3D-CFD simulations. The research was combined to compare the 10%–16% EGR and Miller (effective compression ratio = 8~14.4) strategies respectively in terms of the emissions, efficiency and the local combustion process. The results show that both combustion strategies provide very low NO_x levels below 1 g/kg_{fuel}, which correspond to 0.2 g/kWh. These levels are well below the limit of 0.4 g/kWh imposed by EURO VI regulation.

The above researches have given valuable results; nevertheless, there are also insufficiencies, such as it is difficult for a one dimensional CFD simulation code to predict the in-cylinder combustion process in reference [15], especially for the emissions. In references [16,17], deeper Miller timing over 20°CA BBDC and an EGR rate which is higher than 20% were not presented, and Jesús Benajes confirmed how Miller cycle and EGR strategies are suitable for decreasing simultaneously NO_x and soot emissions down to ultra-low levels, but he did not investigate the combination of these two technologies. For the Tier III emission regulation, NO_x emissions still need to be further reduced if only one of the two technologies is adopted. Moreover, not so many of these kinds of strategies have been carried out on marine diesel engines, especially those which use high boost pressure with Miller cycle, because there are still problems which need to be solved, such as how EGR technology works in conjunction with high turbocharging technology. When using extreme Miller cycle technology, a two-stage turbocharger must be incorporated, this implies that the exhaust pressure will be smaller than the inlet pipe, and thus the traditional EGR circuit connection cannot be simply adopted; also the application of two-stage turbo charging increases the manufacturing costs of the engine. Meanwhile, although a much lower compression terminal temperature is achieved by using an extreme Miller cycle, in the low load condition, a miss fire phenomenon is liable to happen. In addition, overlong ignition delay period, which can be obtained from a decrease of effective compression ratio, promotes the heat release of premixed combustion, and increases the local instantaneous high temperature zones in the cylinder, which weakens the ability of the Miller cycle to reduce NO_x emissions [18].

With the above background, this research considers the technology which combines moderate Miller cycle with moderate EGR rate as a more feasible technical route to realize IMO Tier III regulations. The aim of the current study is to clarify the effects of advancing IVC (intake valve close) angle (Miller cycle 0–70°CA BBDC), boosting the ratio of the charge, enhancing the geometric compression ratio, delaying the injection timing and 0%–30% EGR rates on the performances and emissions of a medium speed marine diesel engine, shown as in Figure 2. This is achieved by means of the combination of one and three dimensional (1D & 3D) Computational Fluid Dynamics (CFD) simulation, using AVL BOOST and FIRE packages respectively. The whole engine performance model was established by 1D CFD software to provide the initial in-cylinder temperatures and pressures for 3D CFD simulations. The influence of Miller cycle and EGR technologies on the compression terminal temperature and pressure can be taken fully into account, while the in-cylinder combustion process and emissions are simulated by 3D CFD software.

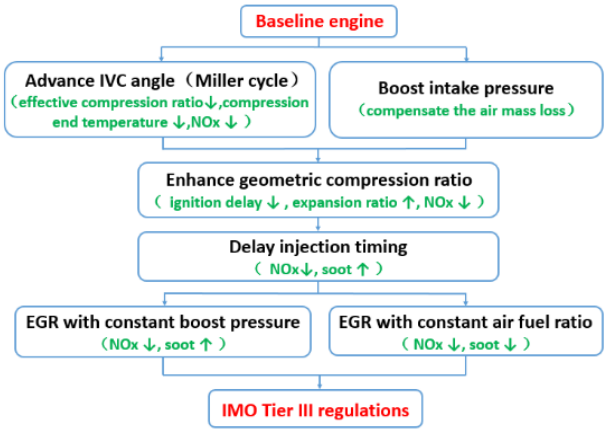

Figure 2. IMO Tier III technology roadmap.

2. Models and Validation

The research was performed on a medium-speed turbocharged diesel engine. Specifications of the engine are listed in Table 1. Combined experiments and 1D & 3D CFD simulations were performed in the study. Bench experiments of the prototype engine were conducted to obtain the performance and emission data, as well as in-cylinder pressures at different loads. These data were used to validate 1D & 3D CFD models. The 1D CFD simulations were carried out to assess the effects of different Miller valve timings on engine performance, as well as to match the proper parameters for two-stage turbocharging systems and intercoolers. Additionally, the results of 1D CFD simulation can provide initial conditions for 3D CFD simulations, which were performed to investigate the in-cylinder combustion and emissions formation processes under Miller cycle conditions.

Table 1. Parameters of the engine.

Items	Parameters
compress ratio	12.4
bore*stroke (mm)	240*275
rated speed ($r \cdot min^{-1}$)	1000
chamber shape	ω
injection timing (°CA ATDC)	−12
piston offset (mm)	74

Figure 3 shows the connection of the experimental instruments. In the process of diesel engine operation, the speed, cylinder pressure and oil signals are acquired through the corresponding sensors, and transferred to the host of combustion analyzer. The corresponding curves and data are the output of the displayer after processing. The AVL-Indiset 620 combustion analyzer is used for the measurement of in-cylinder pressure and the calculation of rate of heat release rate.

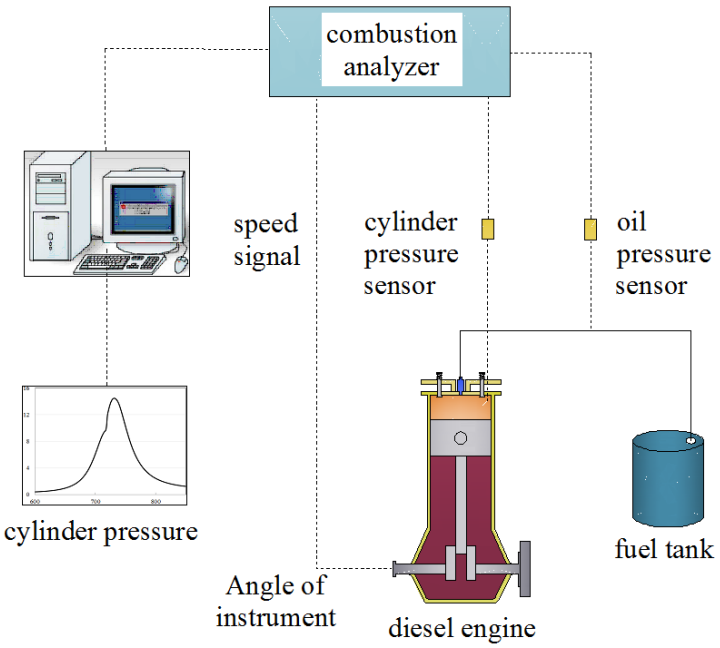

Figure 3. Connection of the experimental instruments.

2.1. One-Dimensional CFD Model

The 1D CFD model built in AVL Boost software is showed in Figure 4. Only the part outside the dotted box is used for the process of model verification and validation. The construction of the diesel engine is composed of two independent air inlets, outlets, and two sets of turbochargers and inter-coolers which are equipped at both ends of the engine. The engine was arranged as a V-type with 16 cylinders which share one inlet and one exhaust manifold. The model includes two-stage turbocharging and external EGR circuit. Since the exhaust back pressure is higher than the intake boost pressure in a turbocharged diesel engine, the auxiliary equipment, such as air blower, supercharge, Venturi tube and so on, need to be arranged in the external EGR route to increase the pressure, and make sure that the recirculated exhaust gas can pass into the intake air pipe successfully. Two turbochargers, TCP1 and TCP2, were put in the model to simulate the above process in this study, as shown in Figure 4.

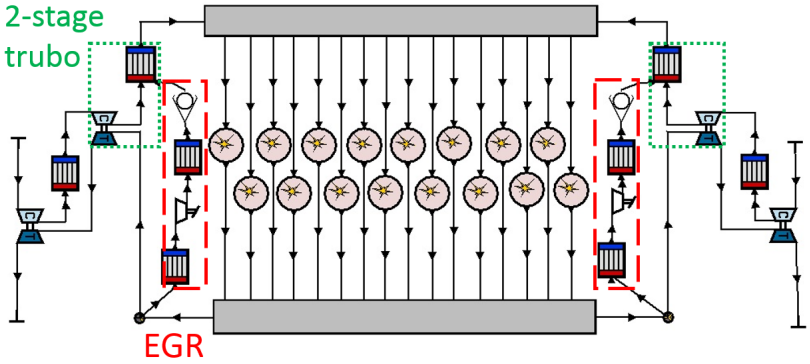

Figure 4. Computational model.

Firstly, the whole engine working process in the test cycle E3 was calculated, and the specific conditions of the test cycle are listed in Table 2. The reliability of the simulation model was validated according to the bench test data.

Table 2. Test cycle E3 for a 16V240 diesel engine.

Test cycle E3	1	2	3	4
power/kW	3240	2430	1620	810
speed/r·min^{-1}	1000	910	800	630

The comparison between the experimental and numerical data of the main performance parameters under the rated conditions are shown in Table 3. The results show that the maximum deviation between the experimental and numerical results is less than 1%, and the deviation between the simulated temperature both before and after the turbine and the experimental data is in the permitted range. When simulating the work process in low and medium load, the deviation still remains below 4%, but the computed maximum pressure is slightly higher than the experimental data, and the deviation range is within 6 bar. On consideration of the cylinder pressure loss in the experiments, the numerical results can be accepted. The established model can predict the performance of the diesel engine with reasonable precision.

Table 3. Comparison of the performance parameters between experimental and simulative data under rated conditions.

Items	Experiment	Simulation	Error
P_e/kW	3240	3240	0.0%
P_{max}/bar	155.1	154.6	0.3%
BSFC/(g/kWh)	207	207.1	0.0%
BMEP/bar	1.943	1.957	0.7%
T after intercooler/K	315	315	0.0%
turbocharge ratio	3.5	3.5	0.0%
Inlet manifold flow/(kg/s)	3.3–3.6	3.4	✓
T before turb/K	756 (±20)	768.1	✓
T after turb/K	592 (±20)	597.1	✓

* BSFC:brake specific fuel consumption; BMEP: brake mean effective pressure.

2.2. Three-Dimensional CFD Model

Because the general 1D CFD computation can hardly predict NO_x emissions accurately, a three-dimensional CFD model of the diesel engine which was established by AVL Fire software is needed. A fast and steady grid formation process can be realized through automatic grid technology based on the octree process using AVL Fire software, and such grid formation arithmetic is insensitive to the surface quality. The nozzle of the experimental diesel engine is arranged in the center, and eight nozzle holes are distributed along the peripheral direction symmetrically. A 1/8 cylinder model has been used to simulate the combustion process of the spray from one nozzle hole, so as to save computation time. The simulation range is 580–850°CA (IVC-EVO). Figure 5 shows the computational grid at TDC (top dead center), and the total number of the grid is 25669 at this time. Before the simulation research, four different sizes of the grid were studied to observe from the results the sensibility to the grid; the grid sizes in the vertical section are 1, 2, 3 and 4 mm respectively. Comparing the in-cylinder pressure curves simulated by four kinds of grids, well fitness can be seen during the compression process, but this is different when the combustion starts. The maximum cylinder pressure decreases with the reduction of the grid size. However, when the grid is reduced to 2 mm, the calculation results tend to be stable. Finally, a 2 mm grid was used to simulate the combustion process in this research. Moreover, a "rezone" method which is provided by Fire is adopted to adjust the size of the moving grid with different crank angles.

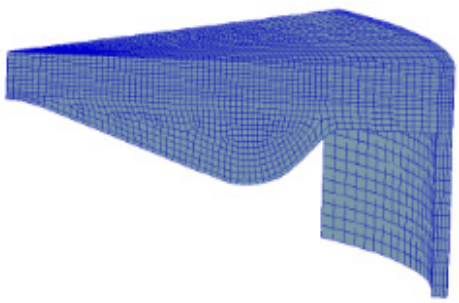

Figure 5. Computational grid of combustion chamber at TDC (top dead center).

In the three-dimensional simulation, the k-ζ-f four equation models were used to close the RANS equation [19]. Hybrid wall function was adopted to deal with the wall boundary layer [20]. Spray

breakup was computed with KH-RT model [21]. The spray and wall interaction process was modeled with the Naber-Reitz model [22]. The evaporation of liquid fuel was determined by the Dukowicz model [23]. The interaction between oil particles and the turbulent vortex group was calculated using the Gosman-Ioannides [24] random turbulent diffusion model. The combustion model was the ECFM-3Z model [25], which can simulate both premixed combustion and diffusion combustion; therefore, it is suitable for combustions in medium speed diesel engines. NO_x emissions were calculated by the Zeldovich model, and soot formation and oxidation were simulated by the Kennedy/Hiroyasu/Magnussen model [26]. It is corrected based on the two step empirical model to predict soot emissions proposed by Hiroyasu. The soot mass fraction Sφ is presented by a conservation equation: $\frac{\partial}{\partial t}(\bar{\rho}\tilde{\phi}_s)+\frac{\partial}{\partial x_j}(\bar{\rho}\overline{u_j\tilde{\phi}_s})=\frac{\partial}{\partial x_j}(\frac{\mu_{eff}}{\sigma_s}\frac{\partial \phi_s}{\partial x_j})+S_{\phi_s}$. S_{ϕ_s} represents the soot formation rate, and is the source item in the conservation equation: $S_{\phi_s}=S_n+S_g+S_{O_2}$, S_n represents the crystal nucleus source item, S_g represents the surface source term growth, S_{O2} represents the oxidation of the source term.

Figure 6 shows the comparison between experimental data and simulation results of in-cylinder pressure of the diesel engine. It can be seen that the experimental and numerical curves agree well. In addition, the NO_x emissions data tested from the emission experiment in the test cycle E3 are comprised of the tree-dimensional simulation results, shown in Figure 7. The figure shows that the simulation results can fit the experiment results well under the rated condition; in the low and medium load conditions. The simulation results are lower than the experiment results, but the overall trend can reflect the emissions of the diesel engine. In conclusion, the simulation model has the ability to reasonably predict NO_x emissions in the full load condition range.

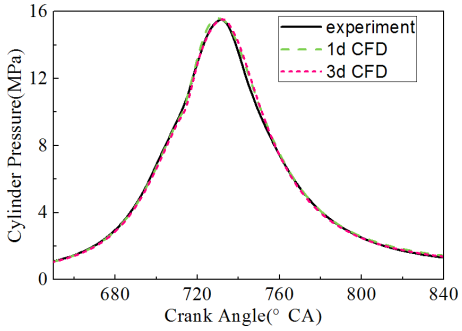

Figure 6. In cylinder pressure curve.

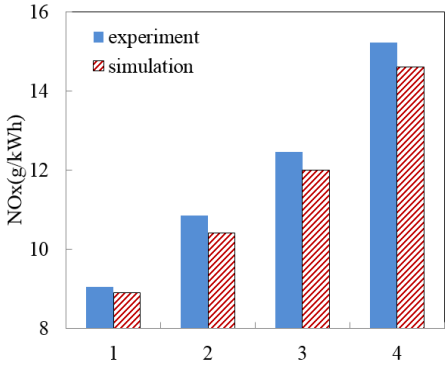

Figure 7. NO_x emissions of E3 test cycle condition compared with simulation data.

3. Results and Discussion

Figure 8 shows the contour images of the fuel/air equivalent ratio, in-cylinder temperature, NO_x, and soot mass fraction of the baseline engine. The formation of diesel engine pollutants shows that soot emissions are produced in the local rich oil mixture where the combustion temperature is higher than 1800 K, and the excess air ratio is lower than 0.5; NO_x emissions are formed in the local high temperature regions with rich O_2, where the combustion temperature is usually higher than 2300 K. The simulation results show the same trend as the above mechanisms. It can be seen that when the in-cylinder temperature increases above 2300 K, the NO_x starts to form near the TDC, and the high NO_x region concentrates in the periphery of the spray during the early injection time (720–730°CA). At the end of fuel injection (740°CA), the NO_x concentration region moves to the pit of the piston. From the figure, the red region of NO_x is transferred to the pit at 740–760°CA, and ϕ is in the range of 0.6–1.2. On the other hand, soot emissions are produced in the center of the spray firstly, and then move to the outskirts of the clearance near the cylinder head. Compared to the NO_x formation region, the soot concentration region appears when the spray impinges the pistion where ϕ is higher than three with the temperature in the range of 1700–2300 K. The last concentration region of soot appears near the cylinder head at 740–750°CA, during this time, the mixture transfers along the piston to the outskirts of the clearance, then turns round when meeting the cylinder wall. The mixture then begins to move up to the cylinder head, so it becomes a rich oil region where ϕ is in the range of 1.4–2.1.

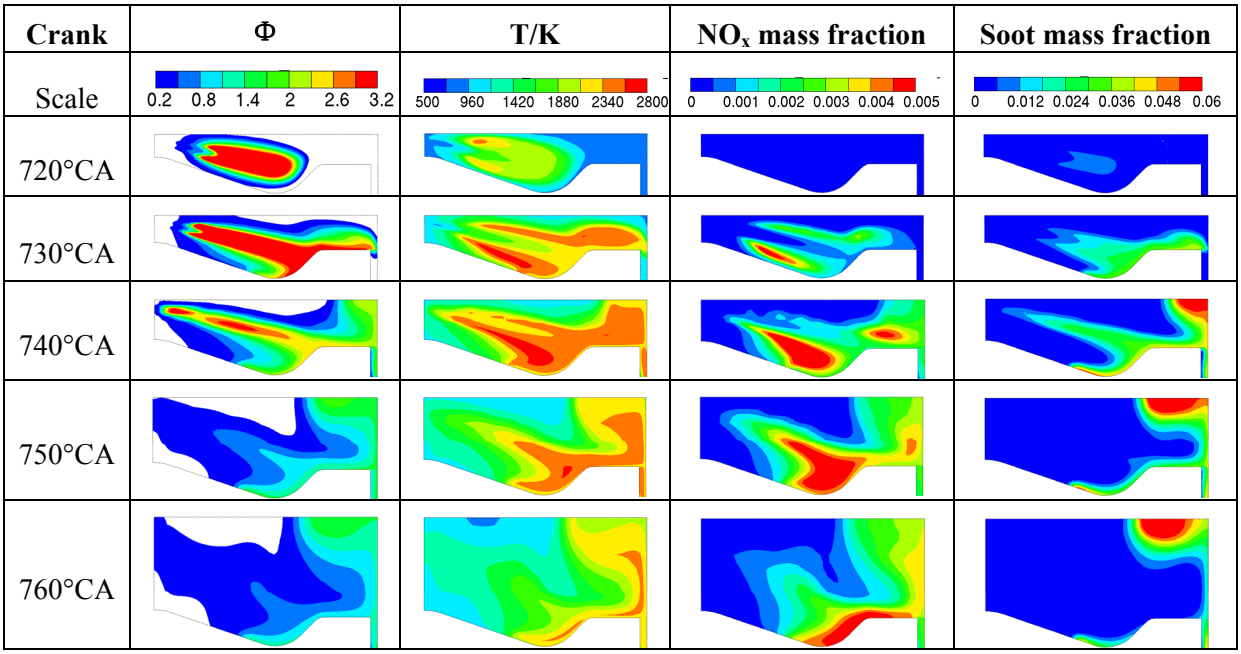

Figure 8. Contour images of equivalent ratio, temperature, NO_x, and soot mass fraction of baseline.

3.1. Effects of Miller Valve Timing

Eight Miller cycle schemes with different advance close timings through 10–80°CA were simulated. The fuel/air equivalence ratio ϕ, intake manifold temperature, and power are kept the same as the baseline engine in this set of simulation. Figure 9 shows the comparison of the effective compression ratio, boost ratio, and in-cylinder temperature at 580°CA (IVC timing of the baseline

engine) between the Miller cycle and baseline engine schemes; the Miller schemes are marked as M+crank angle of the IVC timing advance referring to the BTC; for example, M40 represents the intake valve close timing is 40°CA BBTC. Due to the advance of the inlet valve closing time, the effective compression ratio is reduced. Since there is a 74 mm piston offset, the effective compression ratio of the M40 scheme is a little different from the baseline. The turbochargers with higher boost ratio are required to maintain the same intake air quantity as the baseline engine, so as to avoid the increase of NO_x and thermal load. Two-stage turbocharging was employed in the M60, M70, and M80 schemes. The initial in-cylinder temperature and pressure of different Miller timings at 580°CA that should be inputted into the 3D CFD were obtained from the results of 1D CFD simulation. The in-cylinder temperatures reduce gradually, since the expansion of the endothermic process takes a longer period of time in a deeper Miller cycle, and the temperature at the compression end is also reduced. Consequently, the flame temperature is reduced. There are two key factors in the NO_x formation process: one is high temperature and the other is rich O_2. As one of the above conditions has been suppressed, the NO_x emissions can be reduced.

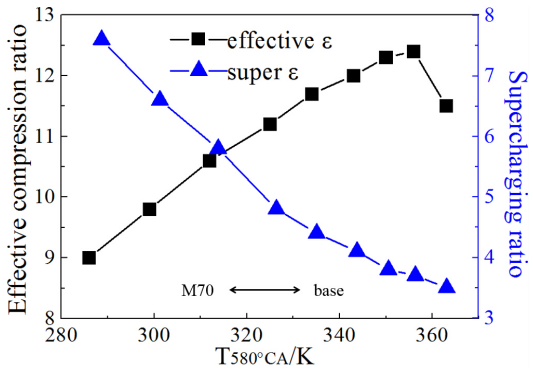

Figure 9. Comparison between Miller and base schemes in effective compression and boost ratios.

A comparison of NO_x and soot emissions under different Miller cycle conditions is shown in Figure 10. The in-cylinder temperature at the compression end time reduces as the intake valve close timing advances, and NO_x emissions decrease substantially. It can be seen that the NO_x was reduced by 27.1% in the M50 scheme. The results show that when the in-cylinder temperature at the intake valve close timing of the baseline engine is kept in the range of 299–312 K in Miller schemes, the normalized NO_x reduction remain at about 27%. On the contrary, if the intake valve closes even earlier, the NO_x emissions increase by 5.8%. This is because the lower compression temperature extends the ignition delay period, then more premixed gas is formed in the longer ignition delay period, and the peak of premixed heat release increases; this was verified by Roel Verschaeren [16]. Since the peak of premixed heat release increases in Miller schemes, the in-cylinder temperature and pressure will increase rapidly in this period. This phenomenon not only leads to rough working possibly, but also weakens the ability to reduce NO_x emission [27]. On the other hand, there is no obvious change in the soot emissions with low degree Miller cycle. The relative change of soot emissions is less than 5% in the M20–40 schemes compared with the baseline engine. When continuing to increase the Miller cycle degree, the compression terminal pressure becomes lower, and there is a retard on the start of combustion timing, since the ignition delay period is longer. The soot emissions can be restrained by the increase of the premixed combustion heat release. The soot emissions were 28.9% lower in the

M50 scheme than for the baseline engine. The start of combustion timing is already delayed after the TDC in the M60 and M70 schemes. The soot emissions are inhibited significantly, and the decreasing rate reached about 85%.

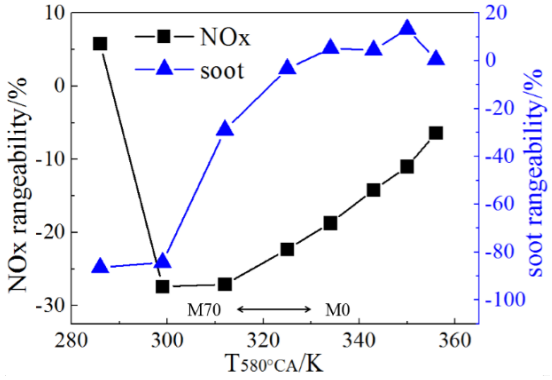

Figure 10. Influence of Miller timing on NO_x and soot.

Figure 11 shows the comparison of the temperature, NO_x and soot mass fraction between the M60 and the baseline scheme. It is obvious that the in-cylinder temperature is reduced when Miller cycle is applied, and the NO_x and soot emissions are reduced dramatically. Since the distribution of ϕ is not changed too much over 740–780°CA, the in-cylinder temperature is the most important factor which determines the formation of NO_x and soot. It can be seen in the figures that the high NO_x region is reduced in the whole combustion process, and only a small red region appears near the piston pit at 740–760°CA. Meanwhile, due to the longer ignition delay, the local fuel/air equivalent ratio decreases, and the reduction range of the soot is even larger. It can be seen from the figure that the red region has disappeared completely. Up to now, NO_x and soot have been reduced by 27.4% and 84.3% respectively by controlling the in-cylinder temperature. It also reflects that the NO_x and soot can be further reduced if the problem of the oil accumulation in the piston pit can be solved. In conclusion, the combination of reducing in-cylinder temperature and organizing the air flow is an effective way to reduce both NO_x and soot.

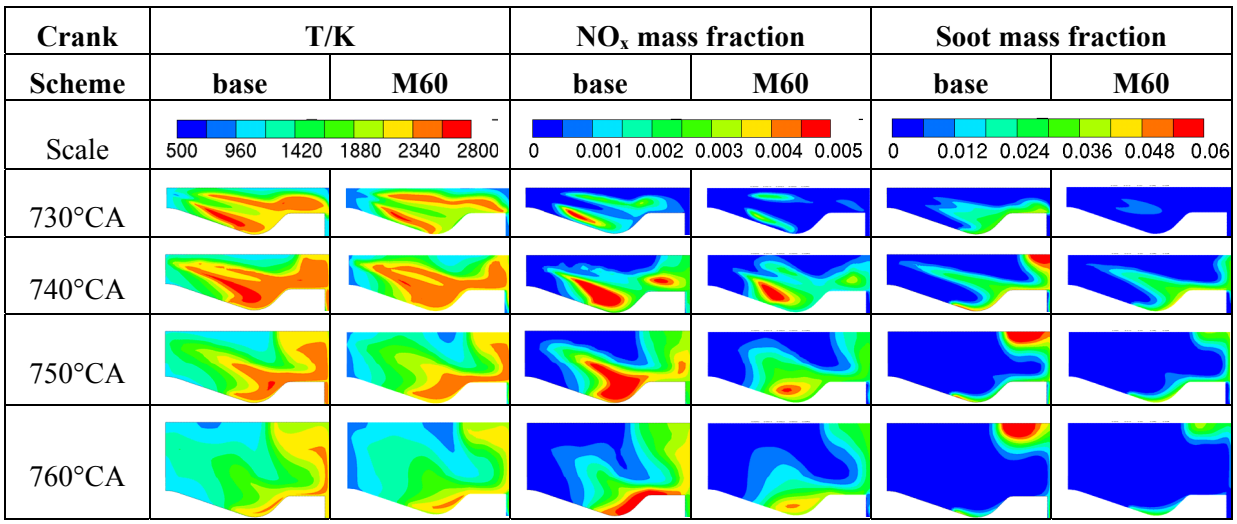

Figure 11. Contour images comparison of temperature, NO_x, and soot mass fraction between M60 and baseline schemes.

Figure 12 shows the effect of Miller valve timing on the maximum cylinder pressure and BSFC (brake specific fuel consumption) compared to the baseline engine. It is obvious from the figure that the maximum cylinder pressure is decreased along with the degree of Miller cycle becoming deeper. The minimum data of maximum cylinder pressure occurs in the M50 scheme, and then increases gradually. This is because the ignition delay period is longer in Miller schemes, and the combustion starting phase is retarded, so the maximum cylinder pressure will decrease with the deeper Miller cycle. Meanwhile, when the total mass of the intake gas is constant, the in-cylinder pressure will decrease with reducing temperature at the same crank angle by the ideal gas state equation. The maximum cylinder pressure shows an increasing trend in the M60-70 schemes because of the pressure explosion which is caused by the multiplied heat release during the premixed combustion. On the other hand, medium Miller cycle has little effect on the fuel economy of the diesel engine, and BSFC is maintained in the baseline engine level. The BSFC is reduced since two-stage turbocharging is used in the M50 scheme. However, due to the overmuch pumping loss, the combustion deteriorates in the M60-70 schemes. Although two-stage turbocharging is also used, BSFC still becomes worse. In view of the whole process of Miller cycle deepening, the premixed heat release peak increases gradually, and the ignition delay period becomes longer. In conclusion, the Miller cycle affects the maximum cylinder pressure to some extent less, and the effect depends on two factors: one is the peak of premixed heat release; the other is the ignition delay period.

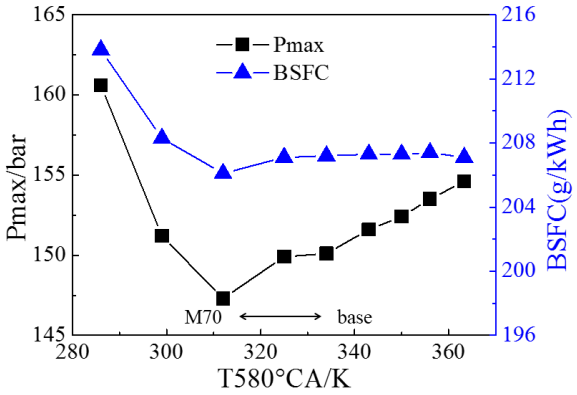

Figure 12. Influence of Miller timing on firing pressure and BSFC (brake specific fuel consumption).

3.2. Effects of High Geometric Compression Ratio

The compression temperature decreases with the deepening of the Miller cycle, and it affects the cold start process of the diesel engine to a certain extent. In order to improve the cold start ability and the fuel economy, and also to weaken the disadvantageous effects of strong premixed heat release in the Miller cycle, the effect of a high geometric compression ratio on the performance and emissions of the Miller cycle diesel engine were numerically analyzed. Retaining the same combustion chamber shape, four high geometric compression ratio Miller schemes were designed by reducing the model's clearance based on the M50 scheme, as shown in Table 4. The baseline M50 scheme is marked as G12.4, and the M50 combined with high geometric compression ratios are marked as G12.4–15.4 respectively. Due to the increase of the geometric compression ratio, to a certain extent, the fuel economy is improved, and further reduction of NO_x can be achieved by retarding the injection timing.

Table 4. Settings and results of high ε Miller cycle.

Scheme	Miller	ε	NO_x	Soot
G12.4	M50	12.4	27.1%↓	28.9%↓
G13.4	M50	13.4	28.8%↓	4.5%↑
G14.4	M50	14.4	36.6%↓	2.9%↑
G15.4	M50	15.4	40.5%↓	21.7%↓

When the geometric compression ratio is enhanced, on the one hand, the expansion ratio can be increased; on the other hand, the premixed heat release peak and the maximum combustion temperature aree reduced, which is beneficial for the reduction of NO_x due to the shorter high temperature period. Such NO_x reduction is obvious, especially in the G15.4 scheme. Thus it can be seen that the desired effect of suppressing the high local in-cylinder temperature during the combustion process has been achieved by enhancing the geometric compression ratio. The thermal efficiency is increased by enhancing the geometric compression Miller schemes, and the fuel economy also benefits. The NO_x decrease ability of the Miller cycle is weakened because of the rapid increase of the local temperature during the premixed combustion period. On the contrary, as there is restriction on the premixed heat release by enhancing the geometric compression ratio, the duration of the high temperature can be shortened effectively, so that the formation of NO_x can also be suppressed. As shown in Table 4, based on the G12.4 scheme, the normalized NO_x emission is increased along with the auxiliary increase of the geometric compression ratio, and the goal of increasing the NO_x reduction ability of the Miller cycle is finally achieved. In the G15.4, the M50 scheme is combined with the high geometric compression ratio which is increased to 15.4, and NO_x is reduced by 40.5%. This improves the NO_x reduction ability of the Miller cycle by 14%, and the soot emissions is 21.7% lower than the base engine.

Figure 13 shows the contours comparison of ϕ, T, NO_x, and soot mass fraction between the G12.4 and G15.4 schemes. It can be seen that ϕ distribution is a little different between G0 and G15.4 because of the reduction of clearance, and the high soot region moves along with the high ϕ concentration at 740–760°CA. Since the ignition delay becomes shorter by increasing the geometric compression ratio, the combustion start point appears earlier in G15.4 than G12.4. In the temperature contour images at 720°CA, a temperature increase which reflects an earlier start of combustion can be observed in the G15.4 scheme, and the red temperature region is always smaller than G12.4 because of the reduction of the premixed combustion heat peak. The high combustion temperature and its duration time are both restrained by decreasing the over high premixed combustion heat peak, while the red NO_x region in G15.4 almost disappears.

Figure 14 shows the effects of the Miller cycle combined with a high geometric compression ratio on the fuel economy and maximum cylinder pressure. The minimum BSFC is obtained in G15.4 in which the fuel consumption is 3.8% lower than the base engine. Further, it is consequent that the maximum cylinder pressure will increase with the enhancement of the geometric compression ratio, so that the mechanical load also increases. Therefore, based on the high geometric compression ratio Miller scheme, the injection time is retarded in the next stage of research, and if it is made sure that the maximum cylinder pressure reduces to the base engine level, the formation of NO_x can be also restrained further.

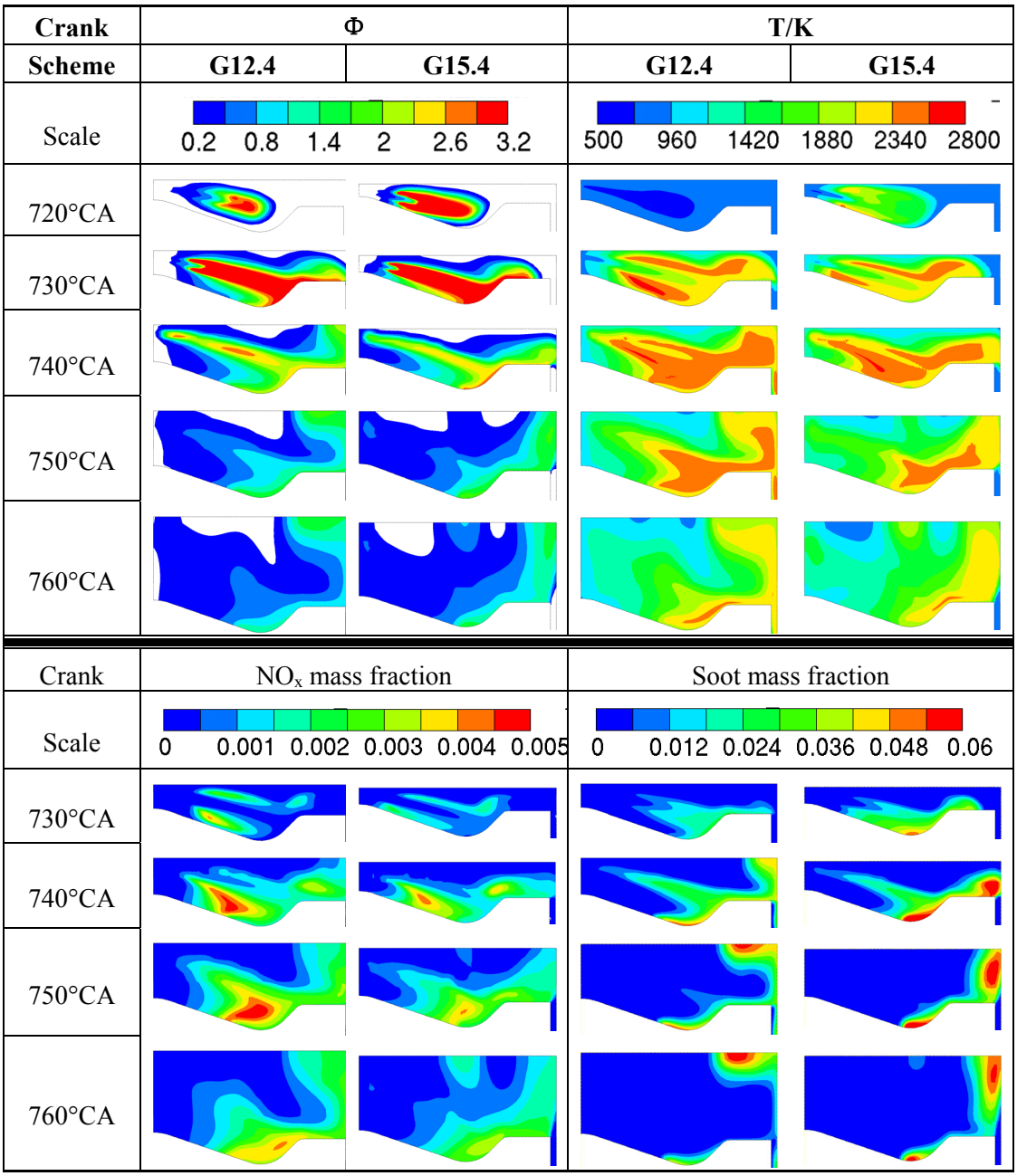

Figure 13. Contour images comparison in Φ, T, NO_x, and soot mass fraction between G12.4 and G15.4.

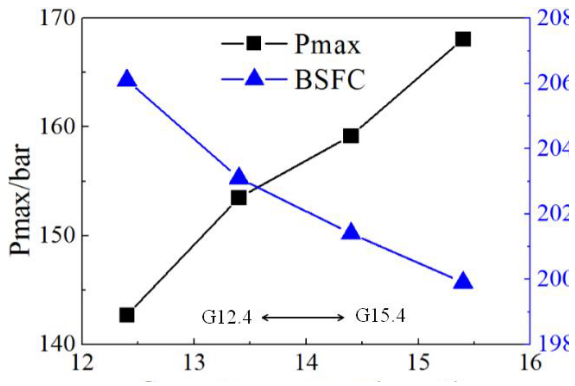

Figure 14. Influence of high ε Miller cycle on maximum cylinder pressure and BSFC.

3.3. Effects of Injection Time

Delaying injection timing is one of the main methods to reduce NO_x, due to the fact that the combustion process transfers to the expansion stroke, resulting in lower combustion flames. Five schemes were simulated in this study, in which the injection time was advanced from −12°CA TDC to −4°CA TDC respectively, as shown in Table 5. The output power was kept constant by adjusting the fuel mass.

Table 5. High ε Miller cycle with different injection times.

Scheme	Miller	ε	Injection /°CA TDC
I12	M50	15.4	−12
I10	M50	15.4	−10
I8	M50	15.4	−8
I6	M50	15.4	−6
I4	M50	15.4	−4

In Figure 15, it can be seen that NO_x emissions are reduced along with the injection delay, but soot emissions increase firstly then decrease with the further injection delay. When the injection timing delays to −4°CA TDC, the NO_x can be reduced by 61.9%, but since the combustion start point appears after the TDC, the maximum cylinder pressure is much lower than the base engine, and the economy relapses back to the base engine level. In the I6 scheme, the NO_x is reduced by 55.6%, meanwhile, the maximum cylinder pressure is just 4.2% lower than the baseline engine, and the fuel economy is 1.8 g/kWh lower. Meanwhile, retarding injection reduces the combustion efficiency, but the influence is very little. It can be seen from the simulation result that the combustion efficiency of the I4 scheme is just 0.2% lower than the I12 scheme.

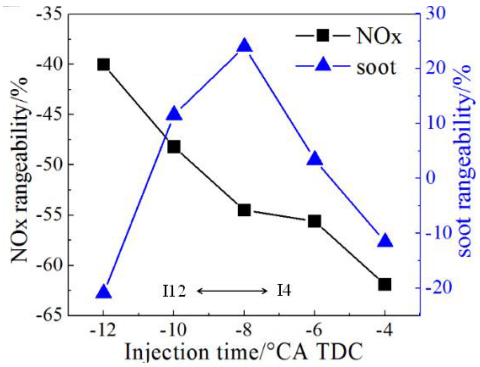

Figure 15. Influence of injection time of high ε Miller cycle on NO_x and soot.

When the extreme Miller cycle is used, the turbocharger should be equipped with a higher pressure ratio, and the cost will increase correspondingly. Meanwhile, the temperature at the intake valve close time decreases drastically with the extreme Miller cycle, and more mixing gas is burnt during the premix combustion due to a longer ignition delay period. The large amount of heat released during premix combustion causes a dramatic increase in temperature, resulting in a large number of NO_x emissions at this stage. Moreover, the overly low temperature at the compression end can cause misfire, and decrease the stability of the diesel engine in the low and medium load conditions; it also can lead to cold start problems. As a result, the combination of medium Miller cycle, high geometric

compression ratio, and delaying injection timing is adopted to reduce NO_x emissions by 50%–60% through taking into account the performance of the diesel engine in the full conditions, while both the power or the fuel economy can remain in the base engine level, and the mechanical load can be reduced to some extent.

3.4. Effects of EGR

In order to further reduce NO_x, high pressure loop cooled EGR is applied in the simulation, as shown in Figure 4, and the output power is kept the same as the baseline engine. Based on the I6 scheme, in which NO_x emissions were reduced 55.3% lower than the base engine, five EGR schemes containing 10%–30% EGR rates were analyzed, as shown as Table 6. The boost ratio of the turbocharger is kept constant in the simulation. With the increase of EGR rate, the O_2 concentration is decreased accordingly, the combustion rate is reduced, as well as the flame temperature. Since one of the key factors which decides the formation of NO_x is the high combustion temperature, the formation of NO_x emissions can be effectively suppressed by reducing the in-cylinder temperature. However,t the soot shows an increasing trend because of the reduction of O_2 concentration caused by EGR.

Table 6. High ε Miller cycle with EGR (exhaust gas recirculation).

Scheme	Miller	ε	EGR rate
E10	M50	15.4	10%
E15	M50	15.4	15%
E20	M50	15.4	20%
E25	M50	15.4	25%
E30	M50	15.4	30%

Figure 16 shows the effect of EGR on emissions with constant boost ratio. The results show that, the NO_x can be reduced by 80% of the base engine if more than 15% EGR is used, which will satisfy the Tier III regulation completely. On the other hand, the soot emissions increase substantially due to the reduction of O_2 concentration caused by EGR rate enhancement. This is the NO_x-soot tradeoff relationship in traditional diesel engine combustion. It can be seen from the figure that the soot emissions continue to increase during the process where the EGR rate increases from 10%–20%. In the E20-E30 schemes in which the EGR rate is over 20%, the amount of soot becomes stable, and the maximum rise is up to 66.3% higher than the base engine. Researches carried out show that reducing in-cylinder temperature can effectively restrain soot formation. Compared with that for the conventional diesel combustion, the number of particles of nucleation mode was increased under the LTC regime, while the mass was reduced [28]. Resultant soot formation including inception and oxidation is reduced due to the in-cylinder combustion temperature decreasing when a large amount of EGR is applied. Although soot emissions can be controlled effectively, the fuel economy is sacrificed. Research data show that the fuel consumption is 3.4% higher when 30% EGR is applied. If even more EGR is adopted in order to further restrain the formation of soot, the combustion process deteriorates, and the fuel consumption will increase obviously. Furthermore, since the combustion rate slows down, the maximum cylinder pressure is also decreased accordingly, and the maximum cylinder pressure of E30 is 3.9 bar lower than E10.

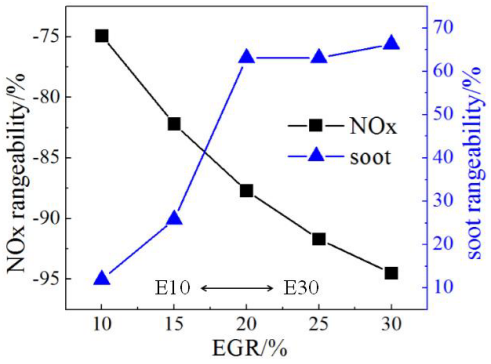

Figure 16. Influence of EGR on emissions at constant boost pressure.

A. Maiboom *et al.* [18] studied the effect of different EGR rates on combustion and emission characteristics on a direct injection diesel engine. The cooled EGR route, variable geometric turbocharger, and intercooler were used in the experiment. The boost pressure was adjusted to keep a constant air fuel ratio. The results show that NO_x is still decreased as the EGR rate increases. The main effect of EGR technology is to dilute the intake gas when boost pressure is kept constant, however soot emissions and fuel consumption increase at the same time. Further, if adjusting the boost pressure to obtain a constant air fuel ratio, the effect of EGR technology then mainly reflects on the temperature effect. Using this method NO_x and soot emissions can be restrained simultaneously, and fuel consumption does not increase. Figure 17 shows the effect of EGR on NO_x and soot emissions in the constant air fuel ratio (2.1) condition which is obtained by adjusting the boost pressure. It can be seen that there is little effect on NO_x by enhancing the pressure ratio of turbocharging, but the soot emissions can be significantly reduced. The soot emissions are 11.4% lower than the base engine when 25% EGR is applied. If the EGR rate is increased to 30%, there is nearly 20% reduction of soot compared to the base engine, so NO_x and soot can be suppressed simultaneously. In this research the output power is kept the same as the baseline in order to judge the emissions at the same reference, so that the BMEP of different schemes was constant. Therefore, although the maximum cylinder pressure is different, the simulation result on IMEP has little change. However, the fuel injection quantity increases at the higher EGR rate. In addition, the fuel consumption, which can be improved by enhancing boost pressure, is just 2.7% higher than the baseline engine in the scheme where 30% EGR is applied, and such raised fuel consumption can be remedied by improving the fuel injection system. Meanwhile, enhancing the injection pressure is also a solution to further reduce soot.

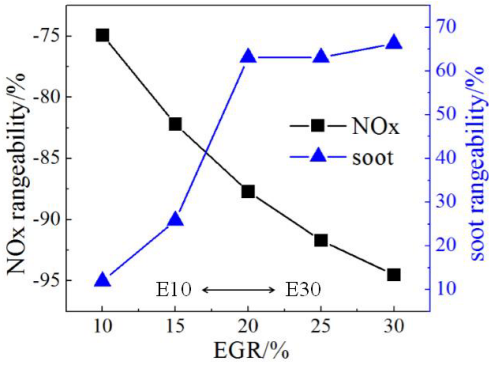

Figure 17. Influence of EGR on emissions at constant excess air ratio.

4. Conclusions

In this research a 16V240 middle speed diesel engine was studied under the rating condition (1000 rpm, 3240 kW). The 1D&3D CFD simulations were both established to simulate the working performance and the in-cylinder combustion process respectively, and different Miller timing, geometric compression ratios, retarding injection, and EGR technology were analyzed. The conclusions are as follows:

(1) The in-cylinder temperature and pressure both decrease at the same crank angle with advanced intake valve close timing (Miller cycle), which cause NO_x emissions to be reduced by as much as 27%.

(2) The expansion ratio is increased, and the ignition delay period is shortened when enhancing the geometric compression ratio, and NO_x emissions can be further reduced; there is a 50%–60% reduction of NO_x when using the Miller cycle combined with high geometric compression ratio and delay injection with the same power and fuel economy of the baseline engine, However the mechanical load is slightly reduced. Moreover, NO_x emission can be reduced more than 80% when over 15% EGR is applied at a constant boost pressure ratio condition. It can satisfy the Tier III regulation, but soot emission and BSFC are increased.

(3) By keeping the excess air coefficient constant, NO_x can be reduced by over 80% when a medium Miller cycle and over 15% EGR is applied, and soot decreases with the boost pressure ratio increase. Soot emissions are nearly 20% lower than the baseline engine, and BSFC is also improved. The optimized scheme (M50, 30%EGR, $\varepsilon = 15.4$, Injection timing = −6°CA TDC) results in an 80% reduction of NO_x, 20% reduction of soot emission，but there is a 2.7% increase of BSFC.

(4) The NO_x and soot emissions can be reduced simultaneously when medium Miller cycle and medium rate EGR technology are applied in the diesel engine. Therefore it is a possible way to meet the IMO Tier III regulations completely. Moreover, compared with the extreme Miller cycle and the high rate EGR technology, this technical route need not be combined with an over high boost ratio, and the economy cost of the diesel engine can be reduced; it also reduces the difficulties of implementation of EGR technology in supercharging diesel engines.

Acknowledgments

Acknowledgment: This research was financially supported by National Natural Science Foundation of China (51479028).

Author Contributions

All the authors have co-operated for the preparation of this work. Shuang He and Wuqiang Long designed research; A final review, including final manuscript revisions, was performed by, Baoguo Du, Liyan Feng, Yao Fu, Jingchen Cui.

Conflicts of Interest

The authors declare no conflict of interest.

References

1. Imperato, M.; Nurmiranta, J.; Sarjovaara, T.; Larmi, M.; Wik, C. Multi-injection and advanced Miller timing in large-bore CI engine. In Proceedings of the CIMAC Congress, Shanghai, China, 13–16 May 2013; Paper No. 157.
2. Nylund, I.; Ott, M. Development of a dual fuel technology for slow-speed engines. In Proceedings of the CIMAC Congress, Shanghai, China, 13–16 May 2013; Paper No. 284.
3. Duong, J.; Hyvonen, J.; Wellander, R.; Andersson, O.; Richter, M. Visualization of the combustion in Wärtsilä 34SG pre-chamber ignited lean burn gas engine. In Proceedings of the CIMAC Congress, Shanghai, China, 13–16 May 2013; Paper No. 414.
4. Soikkeli, N.; Lehikoinen, M.; Ronnback, K.O. Design aspects of SCR systems for HFO fired marine diesel engines. In Proceedings of the CIMAC Congress, Shanghai, China, 13–16 May 2013; Paper No. 179.
5. Wik, C. Tier III technology development and its influence on ship installation and operation. In Proceedings of the CIMAC Congress, Shanghai, China, 13–16 May 2013; Paper No. 159.
6. Potter, M.; Durrett, R.; Motors, G. Design for compression ignition high-efficiency clean combustion engines. In Proceedings of the 12th Annual diesel engine emissions reduction (DEER) conference, Detroit, MI, USA, 20–24 August 2006.
7. Akihama, K.; Takatori, Y.; Inagaki, K.; Sasaki, S.; Anthony, D.M. Mechanism of the smokeless rich diesel combustion by reducing temperature. *SAE Int.* **2001**, doi:10.4271/2001-01-0655.
8. Kimura, S.; Aoki, O.; Kitahara, Y.; Aiyoshizawa, E. Ultra-clean combustion technology combining a low-temperature and premixed combustion concept for meeting future emission standards. *SAE Int.* **2001**, doi:10.4271/2001-01-0200.
9. Shiraishi, T. A Study on the effect and mechanism of plasma assisted gasoline HCCI combustion by low temperature plasma. In Proceedings of the COMODIA, Fukuoka, Japan, 27 July 2012.
10. Koopmans, L.; Ogink, R.; Denbratt, D. Direct gasoline injection in the negative valve overlap of a homogeneous charge compression ignition engine. *SAE Int.* **2003**, doi:10.4271/2003-01-1854.
11. Kamimoto, T.; Bae, M. High combustion temperature for the reduction of particulate in diesel engines. *SAE Int.* **1988**, doi:10.4271/880423.
12. Rajput, K.; Barman, J.; Goswami, A.; Lakhlani, H. Experimental and simulation study to optimize the venturi throat diameter for effective use of EGR rate to achieve BSIV. *SAE Int.* **2013**, doi:10.4271/2013-01-2739.
13. Lakhlani, H.; Barman, J.; Rajput, K.; Goswami, A. Experimental study of EGR mixture design and its influence on EGR distribution across the cylinder for NO_x-PM tradeoff. *SAE Int.* **2013**, doi:10.4271/2013-01-2743.
14. Kim, Y.; Park, C.; Kim, J.; Min, B. The effect of low temperature EGR and low compression ratio on NO_x reduction for EU6 diesel engine. *SAE Int.* **2013**, doi:10.4271/2013-01-2644.
15. Millo, F.; Bernardi, M.G.; Delneri, D. Computational analysis of internal and external EGR strategies combined with Miller cycle concept for a two stage turbocharged medium speed marine diesel engine. *SAE Int. J. Engines* **2011**, *4*, 1319–1330.

16. Verschaeren, R.; Schaepdryver, W.; Serruys, T.; Serruys, T.; Bastiaen, M.; Vervaeke, L.; Verhelst, S. Experimental study of NO_x reduction on a medium speed heavy duty diesel engine by the application of EGR (exhaust gas recirculation) and Miller timing. *Energy* **2014**, *76*, 614–621.
17. Benajes, J.; Molina, S.; Novella, R.; Belarte, E. Evaluation of massive exhaust gas recirculation and Miller cycle strategies for mixing-controlled low temperature combustion in a heavy duty diesel engine. *Energy* **2014**, *71*, 355–366.
18. Maiboom, A.; Tauzia, X.; Hetet, J.F. Experimental study of various effects of exhaust gas recirculation (EGR) on combustion and emissions of an automotive direct injection diesel engine. *Energy* **2008**, *33*, 22–34.
19. Hanjalic, K.; Popovac, M.; Hadziabdic, M. A robust near-wall elliptic-relaxation eddy-viscosity turbulence model for CFD. *Int. J. Heat Fluid Flow* **2004**, *25*, 1047–1051.
20. Huh, K.Y.; Gosman, A.D. A phenomenological model of diesel spray atomization. In Proceedings of the International Conference on Multiphase Flows, Tsukuba, Japan, 24–27 September 1991.
21. Naber, J.D.; Reits, R.D. Modeling engine spray wall impingement. *SAE Int.* **1988**, doi:10.4271/880107.
22. Dukowicz, J.K. A particle-fluid numerical model for liquid sprays. *J. Comp. Phys.* **1980**, *35*, 229–253.
23. Launder, B.; Rodi, W. The turbulent wall jet measurements and modeling. *Ann. Rev. Fluid Mech.* **1983**, *15*, 429–459.
24. Gosman, A.D.; Ioannides, E. Aspects of computer simulation of liquid-fueled combustors. *J. Energy* **1983**, *7*, 482–490.
25. Colin, A.; Benkenida, A. The 3-Zones extended coherent flame model (ecfm3z) for computing premixed/diffusion combustion. *Oil Gas Sci. Technol.* **2004**, *59*, 593–609.
26. Hiroyasu, H.; Kadota, T.; Arai, M. Development and use of spray combustion modeling to predict diesel engine efficiency and pollutants emissions. *Bull. JSME* **1983**, *26*, 569–575.
27. Musculus, M.P.B. On the correlation between NO_x emissions and the diesel premixed burn. *SAE Int.* **2004**, doi:10.4271/2004-01-1401.
28. Jung, Y.; Qi, D.; Bae, C. Assessment of soot particles in an exhaust gas for low temperature diesel combustion with high EGR in a heavy duty compression ignition engine. *SAE Int.* **2013**, doi:10.4271/2013-01-2572.